

# On the Stability and Formation of Pillar[*n*]arenes: a DFT Study

Han Zuilhof,\* Andrew C.-H. Sue, and Jorge Escorihuela\*

Cite This: *J. Org. Chem.* 2021, 86, 14956–14963

Read Online

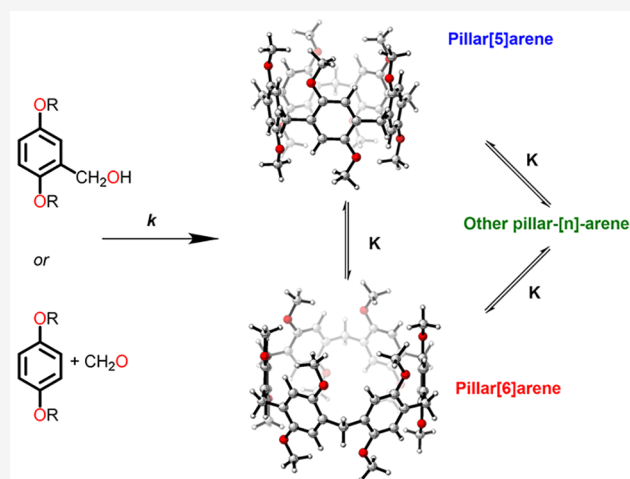
ACCESS |

Metrics & More

Article Recommendations

Supporting Information

**ABSTRACT:** The increased use of both pillar[5]arenes and pillar[6]arenes, stimulated by increasingly efficient syntheses of both, has brought forward the question as to what drives the intermediates in this Friedel–Crafts ring formation to form a pillar[5]arene, a pillar[6]arene, or any other sized macrocycle. This study sets out to answer this question by studying both the thermodynamics and kinetics involved in the absence and presence of templating solvents using high-end wB97XD/6-311G(2p,2d) DFT calculations.



## INTRODUCTION

The rapid rise of supramolecular chemistry has invoked a wide range of macrocyclic compounds,<sup>1</sup> which increasingly make use of the precisely balanced covalent and non-covalent forces. This development has led to classical studies of crown ethers, cyclodextrins, and calixarenes but, more recently, also to a much wider variety, including cucurbiturils, heteroatom-containing macrocycles, and bis-paraquat-based macrocycles.<sup>2</sup> Here, a central theme is relevant, namely, the intrinsic tendency of ring-closing reactions to form smaller rings or linear oligomers, rather than larger macrocycles. The balance between entropy (focusing on easy-to-form small rings or highly disordered oligomers) and enthalpy (often thought to dominate the formation of intermediate size rings) does in such cases tend to optimize specifically sized macrocycles.

A case in point is pillar[*n*]arenes [hereafter referred to as *Pns*]. Discovered by Ogoshi's group in 2008, this class of macrocycles is dominated by the name-giving pillar[5]arenes [*PSs*].<sup>3</sup> With this size, the *para*-substituted aryl rings are all oriented in the same direction (see Figure 1), giving rise to a unique hollow pillar shape. As a result of this structure and because of the ease to construct this macrocycle from intermediate oligomers, it has become one of the pillars of modern macrocyclic chemistry. This development hinges on possibilities for the precise functionalization of *Pns*, which after initial studies of especially mono- and difunctionalized *Pns*,<sup>4</sup> has recently come to full fruition by the development of synthetic methods that allow the functionalization at will of rim-differentiated *Ps*,<sup>5</sup> culminating in the formation of so-

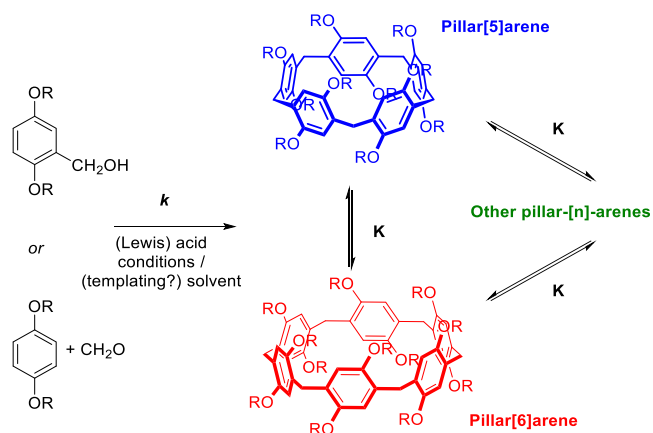


**Figure 1.** Aim of this study: (a) study of thermodynamics of differently sized pillararenes ( $n = 4-8$ ); (b) study of kinetics of pillar[5]arene and pillar[6]arene formation, and (c) the role of templating solvents.

called tiara[5]arenes that are fully functional on one rim, while the other rim consists of C–H moieties.<sup>6</sup> Such improved

Received: July 14, 2021

Published: October 22, 2021



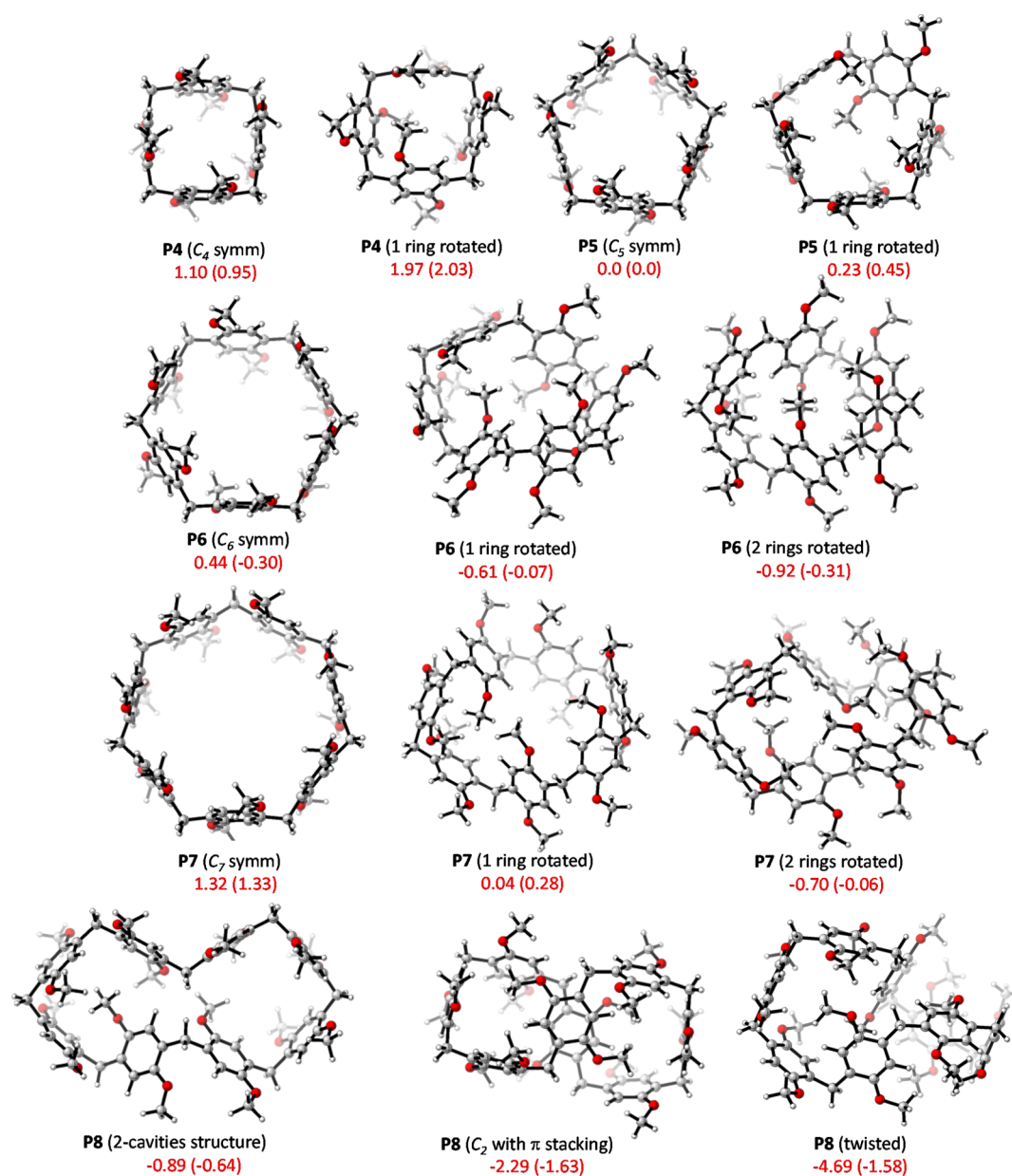


**Figure 2.** Conformations of different sized pillararenes ( $n = 4-8$ ) and relative stability ( $E + ZPE$ ) of these pillar[ $n$ ]arenes *per monomer* compared to P5 (in kcal/mol). Note:  $E + ZPE$  is calculated at the wB97XD/6-311G(2d,2p) level *in vacuo* and in ACN (in brackets).

syntheses have given rise to the development of a wide range of functional P5s that display tailor-made complexation—for example, biosensing—or structural features that allow for the formation of larger aggregates and even steered the discovery of novel phenomena, such as non-porous adaptive crystals, that selectively bind materials but without involvement of the macrocyclic pore.<sup>7</sup> More recently, there is also an increasing focus on P6-based materials.<sup>8</sup> The yield of P6s is characteristically only a few percent in this Friedel–Crafts-based cyclization reaction, but this can be optimized *via* a variety of synthetic approaches, explicitly including changes in the solvent and/or Lewis acid.<sup>9</sup> As a result, more and more P6-based materials have shown up in literature.<sup>10</sup> In contrast, no P4 has been described, and the syntheses of larger P $n$  (P7–P10) have been marred by very low yields.<sup>11</sup>

There are three questions we aim to answer in this paper: (a) to which degree do the thermodynamics of the products

determine the outcome of this ring-forming reaction? (b) Do the different sized P $n$ s display significant differences in their formation, that is, in the corresponding transition states (TSs)? (c) What is the role of the solvent? Given the Friedel–Crafts nature of this reaction, we focus for the latter two questions on the protonated species that actually form the macrocycle. We study these phenomena by high-end range-separated density-functional wB97XD/6-311G(2d,2p)<sup>12</sup> calculations on *per*-methoxy substituted P $n$ s. This combination of a high-end density functional and extensive basis sets creates an approach that can give a proper description of both strain effects in products, intermediates, or TSs, and of the complexation of templating solvent molecules that have been described to play a crucial role in steering the reaction outcome.<sup>13</sup> All DFT calculations were performed using the Gaussian 16 suite of programs,<sup>14</sup> using the solvation model based on density

(SMD) model for generic solvent effects, with acetonitrile (ACN) as a standard solvent.<sup>15</sup>

## RESULTS AND DISCUSSION

**Relative Energies of Pillar[*n*]arenes.** To obtain detailed insights into the thermodynamics of **P<sub>*n*</sub>** formation, we calculated the structures and stability [(here defined as the sum of electronic energy + zero-point energy (*E* + ZPE)] of the four- to eight-membered ring compounds of this family (see Figure 2). For all, a molecular mechanics-based conformational search was performed using the Merck molecular force field in Spartan.<sup>16</sup> While it was not the goal to undertake an extensive conformational search, this approach certified that we did not miss any low-energy conformation. This was then followed by the wB97XD-based DFT calculations. Most of the **P4** and **P5** conformers found in the conformational search were not found as local minima when optimized at the wB97XD/6-311G(2d,2p) level of theory but rather merged into the characteristic symmetric structures, respectively, with *C*<sub>4</sub>- and *C*<sub>5</sub>-rotational axes for the **P4** and **P5** rings, respectively. One other conformer was found in both cases but for both at a higher energy than the name-giving symmetrical ones.

If a ring in the structure is rotated, the energy goes up. For **P4**, this yields (see Figure 2) an energy increase of *ca.* 1 kcal/mol per monomer, that is, 4 kcal/mol, in total. For **P5**, only one low-energy conformer is found (see Figure 2), as confirmed by a recent extensive study of the rotation of **P5** rings.<sup>17</sup> Analogous *C*<sub>6</sub> and *C*<sub>7</sub> symmetric structures are also found for **P6** and **P7**, respectively, but therein the conformational freedom is larger, and the highly symmetric structures do not correspond to the lowest-energy minima: if one or two of the aryl rings are rotated, other conformational minima are also found, and these are even more stable than the more symmetric counterparts by several kcal/mol. The *C*<sub>7</sub> symmetric structure of **P7** also clarifies why that is the case (see Figure 2, bottom left): although the *C*<sub>7</sub> structure is a certified minimum on the potential energy surface (*i.e.*, it displays no imaginary vibrational frequencies), it is characterized clearly by a slight outward bending of the CH<sub>2</sub>-aryl-CH<sub>2</sub> fragments, giving rise to ring strain. In addition, upon changing the rotation of the rings, a more compact structure with increased intramolecular interactions is obtained. The attractiveness of such interactions becomes clear in **P8**, for which no *C*<sub>8</sub> symmetric structure could be obtained. Three different structures were found: a “double cavity” structure that resembles a structure observed in crystals (Figure 2, bottom, left);<sup>11c</sup> a more compact, but still two-fold symmetric structure in which the increasing flexibility in the ring is used to obtain a variety of intramolecular stabilizing interactions, including a slightly tilted  $\pi$ - $\pi$  stacking of the 1- and 5-aryl rings in this molecule (smallest C-C distance: 3.52 Å; full range: 3.52–3.93 Å; Figure 2, bottom, middle); and—as the lowest-energy conformation—a twisted “two-cavity” structure without obvious symmetry elements and significant intramolecular interactions.

Apart from the relative energy of various conformations, the most surprising result obtained from these calculations of various macrocycles actually is the relative stability per monomer. Such comparison reveals the relative stability of different **P<sub>*n*</sub>** members, that is, the relative enthalpy of formation. These data allow us to arrive at four conclusions: (1) **P5** is by far the easiest member to synthesize, but it is not the most stable pillar[*n*]arene. While it is, per monomer,

indeed more stable than centrosymmetric **P4** and **P6** conformers, there are already other **P6** conformers that are more stable per repeating unit. Also, **P7** has a conformation that is more stable, and this is even more the case for **P8**. (2) The 2.29 kcal/mol per monomer, for example, the *C*<sub>2</sub>-symmetric structure of **P8** actually refers to a large stability difference, as it means that when eight **P5** molecules are rearranged to yield five **P8** *C*<sub>2</sub>-symmetric molecules, such a conversion has a reaction enthalpy of 40 × −2.29 = *ca.* −91 kcal/mol. Thus, the enthalpy of the ring closure of diphenol moieties with formaldehyde (or derivatives thereof) itself cannot be the driver for the efficient reaction observed for **P5** formation, and the near-complete lack thereof, for example, **P8**. (3) The name-giving pillar-like structure is a viable structure for the smaller members, but not for any larger ones and then non-pillar-like structures are actually more stable in line with experimental findings. This is perhaps no surprise for **P7** and **P8**, but it is already calculated to be the case for **P6**. (4) While no reports of **P4** have been published, these stability calculations suggest that the strain energy should not be prohibitive in achieving this goal—as already suggested by the successful syntheses of [1.1.1]paracyclophane and pillar[4]-pyridinium<sup>18</sup>—although the role of the solvent in **P4** formation may be a critical one (*vide infra*).

**Ease of Formation of Pillar[*n*]arenes without Templating Solvents.** After concluding that the enthalpy of the ring closure of (formally) diphenol compounds and formaldehyde by itself cannot guide the macrocycle formation, we next focused on the barriers of formation, both in the absence and in the presence of any templating solvent molecules in the (forming) cavity. In the ring closure under Friedel–Crafts conditions, the TS without a templating solvent can be depicted as in Figure 3. In forming the TS, a delocalized

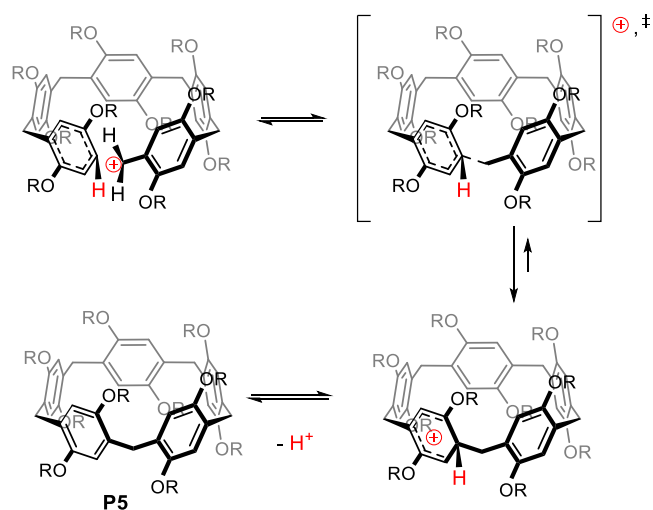


**Figure 3.** Mechanistic steps for ring closure in the formation of pillar[*n*]arenes (indicated here for **P5**); departing H and positive charge are given in red for clarity.

benzylic cation approaches a neutral aryl group. This requires both the soon departing H atom and the H atoms of the CH<sub>2</sub> moiety to bend away from planarity and forward (see Figure 3, top left). In the TS, the new ring-closing C–C bond is formed, and this leads to the protonated ring-closed intermediate (Figure 3, right bottom). In all the investigated cases, this is a real intermediate, as rapid proton transfer to and from, for

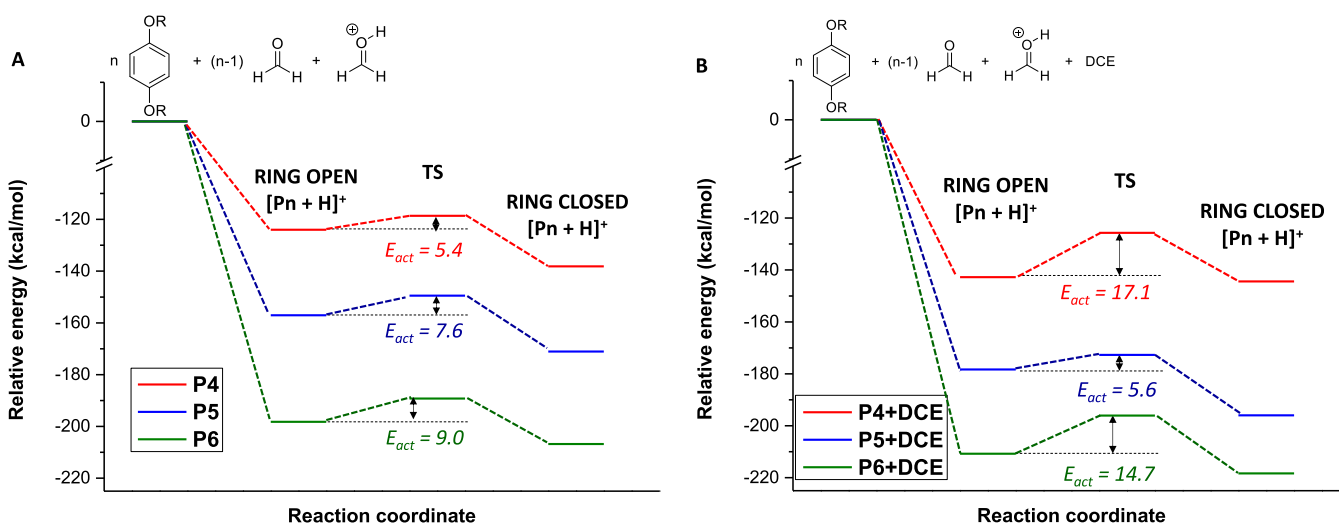


**Figure 4.** Energy diagram (in kcal/mol), in ACN, for the formation of  $P_n$ s and relevant intermediates relative to their reactants: (A) without template and (B) with DCE in the cavity. Note: water molecules formed are not shown for brevity, but  $n$   $H_2O$  is taken into account in calculations.

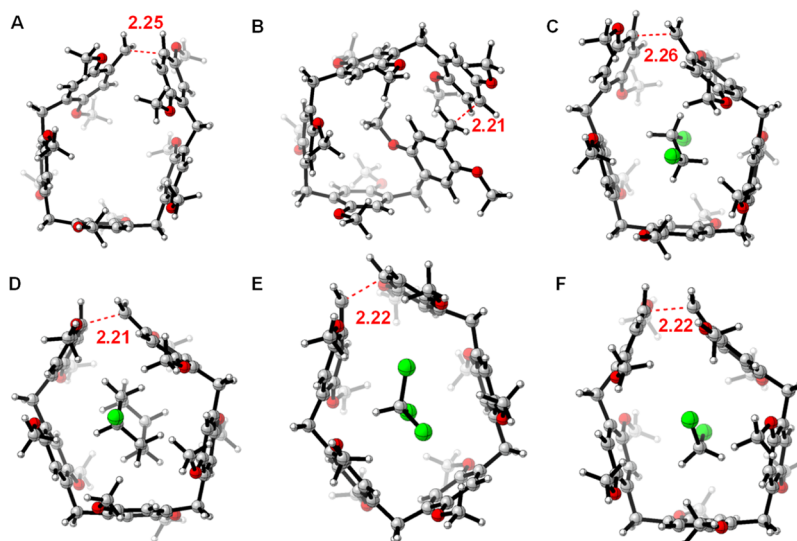


**Figure 5.** TSs for ring-closure to form protonated  $P_5$  (C...C bond-forming distance is given in Å). (A) Nearly  $C_3$  symmetric TS; (B) attack from the inside; and (C–F): TS for  $P_5$  formation with the solvent in cavity, namely, DCE (C), chlorocyclohexane (D),  $CHCl_3$  (E), and  $CH_2Cl_2$  (F).

example, formaldehyde is taking place (e.g.,  $E_{act} = 4.7$  kcal/mol for proton transfer from  $[P_5 + H]^+$  to formaldehyde and  $E_{act} = 3.5$  kcal/mol for proton transfer from protonated formaldehyde to  $P_5$ ). Our computational data shed light on three different facets of the reaction: the overall rate of reaction, the stability of any intermediates and the effects this has on the equilibrium, and the details of the ring formation itself.

To investigate the overall rate, we first calculated the barrier for a non-ring-forming  $P_3$  analogue, so as to remove any component of ring strain (see the Supporting Information for structure). This yielded an activation barrier ( $E + ZPE$  correction) of 3.7 kcal/mol, and within the TS, a typical  $r(C\cdots C) \approx 2.25$  Å. Only slightly higher values for the enthalpic barrier are found for  $P_4$ ,  $P_5$ , and  $P_6$  formation:  $E_{act} = 5.4$  kcal/mol for  $P_4$ , 7.6 kcal/mol for  $P_5$ , and 9.0 kcal/mol for  $P_6$  (see Figure 4, top) These low  $E_a$  values are in line with experimental findings that show that the formation of pillararenes can be efficient at room temperature even without a templating solvent.<sup>19</sup> The overall efficiency of the syntheses is, however, also determined by the stability of the product.

The exothermicity of the cyclization reaction was found to be  $-14.1$  kcal/mol for  $P_4$ ,  $-14.0$  kcal/mol for  $P_5$ , and  $-8.6$  kcal/mol for  $P_6$ . Thus, the experimentally observed ease of formation of  $P_5$ s and  $P_6$ s is in line with these data, but—if this would be the whole story, which it is not (*vide infra*)—the experimental absence of  $P_4$  would still need to be explained.

Second, as a result, the energy barrier from the protonated product to the TS (*i.e.*, the reverse reaction) becomes crucial for the overall yield in the syntheses. The enthalpy of activation for this back reaction was calculated to be 13.4 kcal/mol for the unconstrained  $P_3$  model, 19.6 kcal/mol for  $P_4$ , 21.6 kcal/mol for  $P_5$ , and 17.6 kcal/mol for  $P_6$ . This confirms two things: (1) the ring-forming Friedel–Crafts reaction can indeed be considered as dynamic covalent chemistry with rapid exchange under the commonly used (Lewis) acid catalysis.<sup>20</sup> (2) The (protonated) ring-closed product is thus significantly more stable than the benzylic cation intermediate, clearly driving the reaction in one direction. The low value of the energy barrier for both  $P_5$  and  $P_6$  formation does, however, not imply a simple reaction profile, in which only a

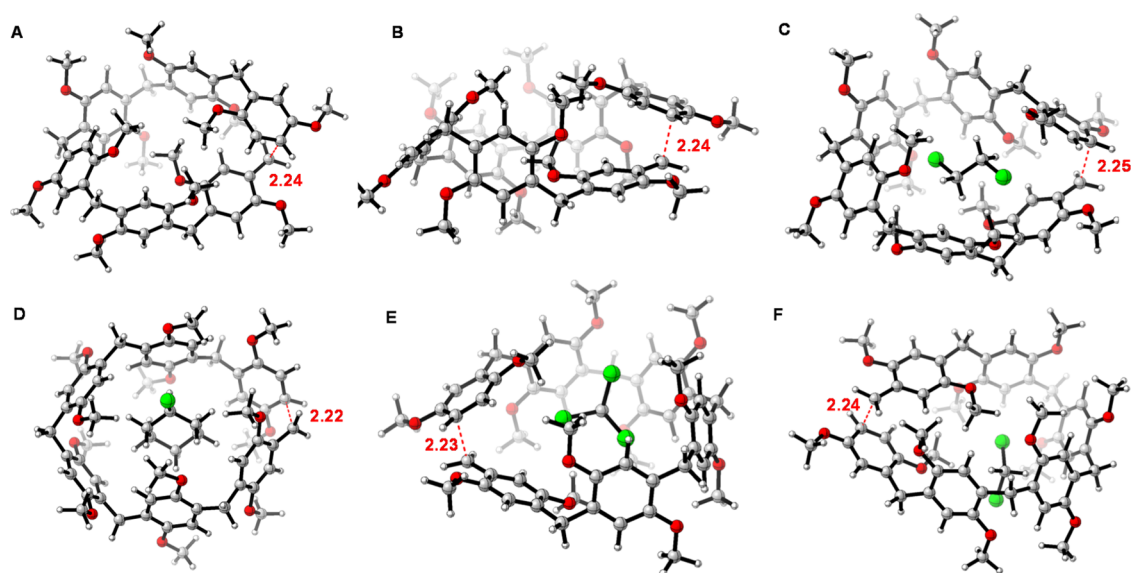


**Figure 6.** TSs for ring closure to form protonated **P6** ( $C\cdots C$  bond-forming distance is given in Å). (A,B) Different views of TSs for **P6** formation; (C–F) TS for **P6** formation with the solvent in cavity, namely, DCE (C), chlorocyclohexane (D),  $\text{CHCl}_3$  (E), and  $\text{CH}_2\text{Cl}_2$  (F).

single path can be followed. For example, when the TS is first approximated by fixing the bond-forming carbon atoms at 2.25 Å (close to the maxima of the  $C-C$  bond-forming potential energy scans for nearly all structures under study) and optimizing the remainder of the structure, then—in the absence of a templating solvent molecule—a “nearly  $C_5$ -symmetric” TS to the protonated **P5** molecule has an activation barrier of 7.6 kcal/mol (Figure 5A). However, an alternative TS can be formed, in which the attacking benzyl cation is attacking “from the inside” with an only slightly higher energy barrier energy ( $E_{\text{act}} = 9.4$  kcal/mol), as shown in Figure 5B. This TS yields a structure in which the H atoms of the bridging point inward, and these then rotate outward in moving from the TS to the protonated **P5** product. This attack “from the inside” proceeded under almost thermoneutral conditions (exothermicity of 2.4 kcal/mol). In other words, while the route indicated in Figure 3 is for **P5**, which indeed is the lowest-energy mechanism, especially for larger macrocycles with increased flexibility, multiple analogous routes would be available.

**Ease of Formation of Pillar[*n*]arenes with Templating Solvents.** All the above energy barrier data only deal with the solvent effects *via* a continuum model that accounts for the polarity and polarizability of the medium surrounding the species, for which we—as a somewhat crude approximation of the evidently heterogeneous mixture of acidic organic solvents—take ACN as the polar organic solvent. However, in the formation of **Pns**, often templating effects of solvents are invoked to explain the relative reactivity and/or product composition that was observed.<sup>21</sup> Therefore, next, the effects of the most frequently used templating solvents [1,2-dichloroethane (DCE), chlorocyclohexane (CyCl), dichloromethane ( $\text{CH}_2\text{Cl}_2$ ), and chloroform ( $\text{CHCl}_3$ )] were investigated.

The cyclization of **P4** with DCE inside the cavity gave a significantly higher barrier of 17.1 kcal/mol with a  $r(C\cdots C) \approx 2.18$  Å (compared to only 5.4 kcal/mol without DCE inside, *vide supra*), and the formation of the protonated product through a nearly thermoneutral reaction (−1.7 kcal/mol). In other words, if **P4** would have a DCE inside, it would lead to a significantly higher barrier than without DCE inside. In fact, a

closer look at the TS and the protonated **P4** product reveals that the DCE lies half outside of the cavity, as it basically cannot fit in it. It is, however, not only the higher barrier imposed by the sterics of a DCE molecule in the cavity (*i.e.*, product destabilization) that hamper the **P4** formation but DCE also stabilizes the reactant: in the ring-opened protonated **P4** intermediate, DCE can be nearly fully wrapped by the tetraaryl cation, yielding a complexation enthalpy of 18.7 kcal/mol. However, such stabilization is nearly given up by the pushing out of DCE from the forming cavity in the ring-closed protonated **P4** (with a complexation enthalpy of only 6.7 kcal/mol). As a result, in DCE and many other cation-stabilizing solvents, rather than helping out, the reactant stabilization effectively fully blocks the formation of **P4**, which explains the near-absence of formation of any **P4**. In addition, it seems likely that only in small-radius, weakly complexing solvents, any **P4** might be producible under such (Lewis) acid circumstances.

The situation for **P5** is more favorable in terms of TS barrier and stabilization of the formed macrocyclic structure. A “nearly  $C_5$ -symmetric” TS could also be obtained with a DCE molecule embedded in the cavity of the forming  $[\text{P5} + \text{H}]^+$  macrocycle (Figure 5C). The role of DCE is frequently referred to as stabilizing the TS by a templating effect.<sup>3b,c</sup>

As now the cavity is filled, only the larger TS can be formed. This yields a barrier of 5.6 kcal/mol, down from 7.6 kcal/mol without DCE in the cavity, and produces the protonated  $[\text{P5} + \text{H}]^+$  macrocycle with an exothermicity of −15.7 kcal/mol. Given the low activation barriers for the formation of the non-cyclic intermediates and for the ring-closure formation of protonated **P5**, these TSs demonstrate that neither any of the non-cyclic intermediates nor the formation of **P5** requires a templating solvent molecule, although the formation is slightly catalyzed by a templating DCE. DCE does, however, also make the formation of ring-closed  $[\text{P5} + \text{H}]^+$  more exothermic (from −14.0 to −17.7 kcal/mol) and thus helps to drive the reaction forward.

In addition, the enthalpy-driven wrapping around DCE by the ring-opened  $[\text{P5} + \text{H}]^+$  implies that the entropic penalty of the ring-closure reaction is likely minimal, certainly compared

to **P5** with DCE in its cavity. Finally, with DCE as a template, the formation of **P5** is strongly favored over both **P4** and **P6** (requiring 17.1 and 14.6 kcal/mol, respectively, see Figure 4B), explaining why it provides access to such smooth high-yielding synthesis.

In contrast, enforcing the reaction involving a templating molecule of CyCl in the cavity of **P5** yielded a TS with an increased barrier of 10.1 kcal/mol and a reaction free energy of only  $-8.3$  kcal/mol (Figure 5D). In other words, CyCl does not properly fit the **P5** cavity and hampers rather than stimulates **P5** formation. Its only positive effect may thus be on the stabilization of any intermediates from outside of the cavity.

The picture becomes more complicated when studying the formation of protonated **P6**. Here, the TS involving a molecule of DCE in the cavity has a barrier of 14.7 kcal/mol and thus 5.7 kcal/mol higher than that without DCE (Figure 6C). Since DCE does not fully fill the cavity, there is still a significant distortion from  $C_6$  symmetry in the TS and no proper activation entropy-lowering pre-organization, although only attack from the outside is observed to lead to the product. In contrast, CyCl really fills the cavity of  $[P6 + H]^+$ , leads to an ordered TS, displays a barrier of only 8.4 kcal/mol, and increases the exothermicity of the ring-closing step from  $-8.6$  with DCE in the cavity to  $-15.0$  kcal/mol with CyCl in the cavity (Figure 6D).

Similar studies were performed with  $CH_2Cl_2$  and  $CHCl_3$  as templates. To validate the accuracy of our theoretical study, we finally compared the calculated barriers for **P5** and **P6** formation in these solvents with experimentally obtained yields of an analogous experimental study by Wang, Rathore, and co-workers, namely, the selective synthesis of **P5** and/or **P6** with methane-sulfonic acid as a catalyst (see Table 1).<sup>22</sup> In

**Table 1. Comparison of Yields and Activation Energies for Pillar[*n*]arene Cyclization with Different Solvents in the Cavity**

solvent	<b>P5</b> yield (%) <sup>a</sup>	<b>P6</b> yield (%) <sup>a</sup>	$E_{act}(\Delta G_R)$ <b>P5</b> <sup>b</sup>	$E_{act}(\Delta G_R)$ <b>P6</b> <sup>b</sup>
DCE	64	trace	5.6 ( $-15.7$ )	14.7 ( $-6.2$ )
$CH_2Cl_2$	71	8	7.2 ( $-12.2$ )	11.8 ( $-8.7$ )
$CHCl_3$	6	79	8.4 ( $-7.7$ )	4.5 ( $-13.4$ )
CyCl	5	56	10.4 ( $-8.3$ )	8.4 ( $-15.0$ )

<sup>a</sup>From ref 22. <sup>b</sup>Activation energies ( $E_{act}$ ) and reaction free energies ( $\Delta G_R$ ) in kcal/mol.

the TSs for **P5** formation, the solvents CyCl and  $CHCl_3$  are actually slightly too big for the cavity, and one and two Cl atoms are slightly above the ring formed by the aryl groups, respectively, thereby providing little stabilizing interactions. With both  $CH_2Cl_2$  and DCE, both Cl atoms are more strongly involved in such stabilizing interactions. For **P6** formation only for CyCl in the cavity, a nearly six-fold symmetric TS is observed. For the other three, the forming ring tries to reorganize in such a manner as to maximize the macrocycle–solvent interactions. For  $CHCl_3$ , such distortion seems to be slightly less qualitatively, as it fills more of the cavity and two of its Cl atoms are directly pointing to an aryl ring. For both  $CH_2Cl_2$  and DCE, such a fit requires more extensive conformational changes of the macrocycle. In all cases, the  $r(C\cdots C)$  is a near-constant, thereby forming a strong limit as to what conformational changes are allowed. In summary, as

observed experimentally, the preferential formation of **P5** in DCE and  $CH_2Cl_2$  and that of the cyclohexamer **P6** in CyCl or  $CHCl_3$  is fully supported by the calculated differences in the activation barriers in each solvent, displaying the potential of our approach.

## CONCLUSIONS

A detailed computational analysis of the process of pillar[*n*]arene formation shows four things: first, the predominance of **P5** in the family of pillararenes is not caused by its intrinsic properties (stability and/or ease of formation)—without an active solvent, **P4** requires a lower barrier to form, and **P7** and **P8** are evidently more stable. Second, while no templating solvents are needed, they do, however, help to slightly reduce the already low activation enthalpy, reduce the activation entropy by pre-wrapping the ring-opened structure around the solvent molecule, and help to drive the reaction forward by their significant complexation energies. Third, it is this solvent–macrocycle interaction that largely determines the relative ease of formation of various pillar[*n*]arenes in different solvents. Fourth, these findings precisely clarify why no **P4** has been formed and also provide guidelines to further facilitate the formation of **P6** and even larger **P<sub>n</sub>** macrocycles. These results not only clarify the current—synthetically successful but conceptually partially vague—factors that drive the pillar[*n*]arene synthesis but also clearly point out the way to search for increased yields of, for example, **P6s**. Analogous analyses can also be made for other macrocycles. The rapidly growing interest in such more extended macrocycles for a variety of novel goals in supramolecular chemistry and materials science thus indicates the potential and experimental feasibility of such detailed mechanistic investigations.

## EXPERIMENTAL SECTION

**Computational Methods.** All DFT geometry optimizations were performed with the dispersion-corrected wB97XD functional and the 6-311G(2d,2p) basis set as implemented within the Gaussian 16 series of programs. Solvent effects were included with the SMD continuum model to mimic ACN during both geometry optimizations and vibrational analysis. All of the energies and enthalpies presented for the reactant complex, TS, and product are given in hartree. All of the energies have been corrected with ZPEs. Vibrational frequency calculations were made at the same level of theory used for optimization. All TSs were verified to have only one negative eigenvalue in the Hessian matrix, describing the motion along the reaction coordinate. Furthermore, the calculated activation enthalpies and reaction enthalpies are given for every reaction in kcal/mol. Optimized structures were illustrated using CYLview20.3.<sup>23</sup>

## ASSOCIATED CONTENT

### Supporting Information

The Supporting Information is available free of charge at <https://pubs.acs.org/doi/10.1021/acs.joc.1c01679>.

Full Gaussian 16 citation, various views for optimized pillar[*n*]arene structures, full results of conformational search, details on complexation energies for pillar[*n*]arenes, and the Cartesian coordinates of all structures in this paper (PDF)

## AUTHOR INFORMATION

### Corresponding Authors

Han Zuilhof – School of Pharmaceutical Science & Technology, Tianjin University, Tianjin 300072, P. R. China;

Laboratory of Organic Chemistry, Wageningen University, Wageningen 6703 WE, The Netherlands; Department of Chemical and Materials Engineering, Faculty of Engineering, King Abdulaziz University, Jeddah 21589, Saudi Arabia; [orcid.org/0000-0001-5773-8506](https://orcid.org/0000-0001-5773-8506); Email: [han.zuilhof@wur.nl](mailto:han.zuilhof@wur.nl)

Jorge Escorihuela – Departamento de Química Orgánica, Universitat de València, Burjassot 46100 Valencia, Spain; [orcid.org/0000-0001-6756-0991](https://orcid.org/0000-0001-6756-0991); Email: [jorge.escorihuela@uv.es](mailto:jorge.escorihuela@uv.es)

## Author

Andrew C.-H. Sue – College of Chemistry and Chemical Engineering, Xiamen University, Xiamen 361005, P. R. China; [orcid.org/0000-0001-9557-2658](https://orcid.org/0000-0001-9557-2658)

Complete contact information is available at: <https://pubs.acs.org/10.1021/acs.joc.1c01679>

## Notes

The authors declare no competing financial interest.

## ACKNOWLEDGMENTS

Financial support from the National Science Foundation of China (grant #21871208) and Wageningen University is greatly acknowledged.

## REFERENCES

- (1) Steed, J. W.; Atwood, J. L. *Supramolecular Chemistry*, 2nd ed.; Wiley-VCH, 2009.
- (2) (a) Crini, G. Review: A History of Cyclodextrins. *Chem. Rev.* **2014**, *114*, 10940–10975. (b) Gutsche, C. D. *Calixarenes, An Introduction*, 2nd ed.; Royal Society of Chemistry: Cambridge, 2008. (c) Barrow, S. J.; Kaser, S.; Rowland, M. J.; Del Barrio, J.; Scherman, O. A. Cucurbituril-Based Molecular Recognition. *Chem. Rev.* **2015**, *115*, 12320–12406. (d) Wang, D.-X.; Wang, M.-X. Exploring Anion- $\pi$  Interactions and Their Applications in Supramolecular Chemistry. *Acc. Chem. Res.* **2020**, *53*, 1364–1380. (e) Liu, Z.; Nalluri, S. K. M.; Stoddart, J. F. Surveying macrocyclic chemistry: from flexible crown ethers to rigid cyclophanes. *Chem. Soc. Rev.* **2017**, *46*, 2459–2478.
- (3) (a) Ogoshi, T.; Kanai, S.; Fujinami, S.; Yamagishi, T.-a.; Nakamoto, Y. *para*-Bridged Symmetrical Pillar[5]arenes: Their Lewis Acid Catalyzed Synthesis and Host-Guest Property. *J. Am. Chem. Soc.* **2008**, *130*, 5022–5023. (b) Ogoshi, T.; Demachi, K.; Kitajima, K.; Yamagishi, T.-a. Monofunctionalized pillar[5]arenes: synthesis and supramolecular structure. *Chem. Commun.* **2011**, *47*, 7164–7166. (c) Ogoshi, T.; Yamagishi, T.-a.; Nakamoto, Y. Pillar-Shaped Macrocyclic Hosts Pillar[n]arenes: New Key Players for Supramolecular Chemistry. *Chem. Rev.* **2016**, *116*, 7937–8002. (d) Ogoshi, T.; Ueshima, N.; Akutsu, T.; Yamafuji, D.; Furuta, T.; Sakakibara, F.; Yamagishi, T.-a. The template effect of solvents on high yield synthesis, co-cyclization of pillar[6]arenes and interconversion between pillar[5]- and pillar[6]arenes. *Chem. Commun.* **2014**, *50*, 5774–5777.
- (4) (a) Al-Azemi, T. F.; Mohamad, A. A.; Vinodh, M.; Alipour, F. H. A new approach for the synthesis of mono- and A1/A2-dihydroxy-substituted pillar[5]arenes and their complexation with alkyl alcohols in solution and in the solid state. *Org. Chem. Front.* **2018**, *5*, 10–18. (b) Strutt, N. L.; Zhang, H.; Schneebeli, S. T.; Stoddart, J. F. Functionalizing Pillar[n]arenes. *Acc. Chem. Res.* **2014**, *47*, 2631–2642. (c) Ogoshi, T.; Aoki, T.; Kitajima, K.; Fujinami, S.; Yamagishi, T.-a.; Nakamoto, Y. Facile, Rapid, and High-Yield Synthesis of Pillar[5]-arene from Commercially Available Reagents and Its X-ray Crystal Structure. *J. Org. Chem.* **2011**, *76*, 328–331.
- (5) (a) Demay-Drouhard, P.; Du, K.; Samanta, K.; Wan, X.; Yang, W.; Srinivasan, R.; Sue, A. C.-H.; Zuilhof, H. Functionalization at Will of Rim-Differentiated Pillar[5]arenes. *Org. Lett.* **2019**, *21*, 3976–3980. (b) Guo, M.; Wang, X.; Zhan, C.; Demay-Drouhard, P.; Li, W.; Du, K.; Olson, M. A.; Zuilhof, H.; Sue, A. C.-H. Rim-Differentiated C<sub>5</sub>-Symmetric Tiara-Pillar[5]arenes. *J. Am. Chem. Soc.* **2018**, *140*, 74–77.
- (6) Yang, W.; Samanta, K.; Wan, X.; Thikekar, T. U.; Chao, Y.; Li, S.; Du, K.; Xu, J.; Gao, Y.; Zuilhof, H.; Sue, A. C. H. Tiara[5]arenes: Synthesis, Solid-State Conformational Studies, Host-Guest Properties, and Application as Nonporous Adaptive Crystals. *Angew. Chem., Int. Ed.* **2020**, *59*, 3994–3999.
- (7) For recent reviews on nonporous adaptive crystals, see: (a) Wu, J. R.; Yang, Y. W. Synthetic Macrocyclic-Based Nonporous Adaptive Crystals for Molecular Separation. *Angew. Chem., Int. Ed.* **2021**, *60*, 1690–1701. (b) Zhou, Y.; Jie, K.; Zhao, R.; Huang, F. Supramolecular-Macrocyclic-Based Crystalline Organic Materials. *Adv. Mater.* **2019**, *32*, 1904824. See further (c) Wu, Y.; Zhou, J.; Li, E.; Wang, M.; Jie, K.; Zhu, H.; Huang, F. Selective Separation of Methylfuran and Dimethylfuran by Nonporous Adaptive Crystals of Pillararenes. *J. Am. Chem. Soc.* **2020**, *142*, 19722–19730. (d) Jie, K.; Zhou, Y.; Li, E.; Li, Z.; Zhao, R.; Huang, F. Reversible Iodine Capture by Nonporous Pillar[6]arene Crystals. *J. Am. Chem. Soc.* **2017**, *139*, 15320–15323.
- (8) (a) Song, N.; Kakuta, T.; Yamagishi, T.-a.; Yang, Y.-W.; Ogoshi, T. Molecular-Scale Porous Materials Based on Pillar[n]arenes. *Chem* **2018**, *4*, 2029–2053. (b) Wang, K.; Jordan, J. H.; Velmurugan, K.; Tian, X.; Zuo, M.; Hu, X. Y.; Wang, L. Role of Functionalized Pillararene Architectures in Supramolecular Catalysis. *Angew. Chem., Int. Ed.* **2020**, *60*, 9205–9214.
- (9) (a) Da Pian, M.; Schalley, C. A.; Fabris, F.; Scarso, A. Insights into the synthesis of pillar[5]arene and its conversion into pillar[6]arene. *Org. Chem. Front.* **2019**, *6*, 1044–1051. (b) Tsuneishi, C.; Koizumi, Y.; Sueto, R.; Nishiyama, H.; Yasuhara, K.; Yamagishi, T.-a.; Ogoshi, T.; Tomita, I.; Inagi, S. The controlled synthesis of pillar[6]arene-based hexagonal cylindrical structures on an electrode surface via electrochemical oxidation. *Chem. Commun.* **2017**, *53*, 7454–7456. (c) Cao, D.; Kou, Y.; Liang, J.; Chen, Z.; Wang, L.; Meier, H. A facile and efficient preparation of pillararenes and a pillarquinone. *Angew. Chem., Int. Ed.* **2009**, *48*, 9721–9723.
- (10) (a) Ueno, M.; Tomita, T.; Arakawa, H.; Kakuta, T.; Yamagishi, T.-a.; Terakawa, J.; Daikoku, T.; Horike, S.-i.; Si, S.; Kurayoshi, K.; Ito, C.; Kasahara, A.; Tadokoro, Y.; Kobayashi, M.; Fukuwatari, T.; Tamai, I.; Hirao, A.; Ogoshi, T. Pillar[6]arene acts as a biosensor for quantitative detection of a vitamin metabolite in crude biological samples. *Commun. Chem.* **2020**, *3*, 183. (b) Ogoshi, T.; Kotera, D.; Fa, S.; Nishida, S.; Kakuta, T.; Yamagishi, T.-a.; Brouwer, A. M. A light-operated pillar[6]arene-based molecular shuttle. *Chem. Commun.* **2020**, *56*, 10871–10874. (c) Zhu, W.; Li, E.; Zhou, J.; Zhou, Y.; Sheng, X.; Huang, F. Highly selective removal of heterocyclic impurities from toluene by nonporous adaptive crystals of perethylated pillar[6]arene. *Mater. Chem. Front.* **2020**, *4*, 2325–2329. (d) Jie, K.; Liu, M.; Zhou, Y.; Little, M. A.; Bonakala, S.; Chong, S. Y.; Stephenson, A.; Chen, L.; Huang, F.; Cooper, A. I. Styrene Purification by Guest-Induced Restructuring of Pillar[6]arene. *J. Am. Chem. Soc.* **2017**, *139*, 2908–2911. (e) Ogoshi, T.; Kida, K.; Yamagishi, T.-a. Photoreversible Switching of the Lower Critical Solution Temperature in a Photoresponsive Host-Guest System of Pillar[6]arene with Triethylene Oxide Substituents and an Azobenzene Derivative. *J. Am. Chem. Soc.* **2012**, *134*, 20146–20150. (f) Yu, G.; Xue, M.; Zhang, Z.; Li, J.; Han, C.; Huang, F. A Water-Soluble Pillar[6]arene: Synthesis, Host-Guest Chemistry, and Its Application in Dispersion of Multiwalled Carbon Nanotubes in Water. *J. Am. Chem. Soc.* **2012**, *134*, 13248–13251.
- (11) (a) Chen, Y.; Tao, H. Q.; Kou, Y. H.; Meier, H.; Fu, J. L.; Cao, D. R. Synthesis of pillar[7]arene. *Chin. Chem. Lett.* **2012**, *23*, 509–511. (b) Chi, X.; Ji, X.; Xia, D.; Huang, F. A Dual-Responsive Supra-Amphiphilic Polypseudorotaxane Constructed from a Water-Soluble Pillar[7]arene and an Azobenzene-Containing Random Copolymer. *J. Am. Chem. Soc.* **2015**, *137*, 1440–1443. (c) Hu, X.-B.; Chen, Z.; Chen, L.; Zhang, L.; Hou, J.-L.; Li, Z.-T. Pillar[n]arenes (n = 8–10)

with two cavities: synthesis, structures and complexing properties. *Chem. Commun.* **2012**, *48*, 10999–11001. (d) Chi, X.; Yu, G.; Shao, L.; Chen, J.; Huang, F. A Dual-Thermoresponsive Gemini-Type Supra-amphiphilic Macromolecular [3]Pseudorotaxane Based on Pillar[10]arene/Paraquat Cooperative Complexation. *J. Am. Chem. Soc.* **2016**, *138*, 3168–3174.

(12) Chai, J.-D.; Head-Gordon, M. Long-range corrected hybrid density functionals with damped atom–atom dispersion corrections. *Phys. Chem. Chem. Phys.* **2008**, *10*, 6615–6620.

(13) Ruengsuk, A.; Khamphaijun, K.; Pananusorn, P.; Docker, A.; Tantirungrotechai, J.; Sukwattanasinnit, M.; Harding, D. J.; Bunchuay, T. Pertosylated pillar[5]arene: self-template assisted synthesis and supramolecular polymer formation. *Chem. Commun.* **2020**, *56*, 8739–8742.

(14) Frisch, M. J.; Trucks, G. W.; Schlegel, H. B.; Scuseria, G. E.; Robb, M. A.; Cheeseman, J. R.; Scalmani, G.; Barone, V.; Petersson, G. A.; Nakatsuji, H.; Li, X.; Caricato, M.; Marenich, A. V.; Bloino, J.; Janesko, B. G.; Gomperts, R.; Mennucci, B.; Hratchian, H. P.; Ortiz, J. V.; Izmaylov, A. F.; Sonnenberg, J. L.; Williams-Young, D.; Ding, F.; Lipparini, F.; Egidi, F.; Goings, J.; Peng, B.; Petrone, A.; Henderson, T.; Ranasinghe, D.; Zakrzewski, V. G.; Gao, J.; Rega, N.; Zheng, G.; Liang, W.; Hada, M.; Ehara, M.; Toyota, K.; Fukuda, R.; Hasegawa, J.; Ishida, M.; Nakajima, T.; Honda, Y.; Kitao, O.; Nakai, H.; Vreven, T.; Throssell, K.; Montgomery, J. A., Jr.; Peralta, J. E.; Ogliaro, F.; Bearpark, M. J.; Heyd, J. J.; Brothers, E. N.; Kudin, K. N.; Staroverov, V. N.; Keith, T. A.; Kobayashi, R.; Normand, J.; Raghavachari, K.; Rendell, A. P.; Burant, J. C.; Iyengar, S. S.; Tomasi, J.; Cossi, M.; Millam, J. M.; Klene, M.; Adamo, C.; Cammi, R.; Ochterski, J. W.; Martin, R. L.; Morokuma, K.; Farkas, O.; Foresman, J. B.; Fox, D. J. *Gaussian 16*, Revision B.01; Gaussian, Inc.: Wallingford CT, 2016.

(15) (a) Marenich, A. V.; Cramer, C. J.; Truhlar, D. G. Universal Solvation Model Based on Solute Electron Density and on a Continuum Model of the Solvent Defined by the Bulk Dielectric Constant and Atomic Surface Tensions. *J. Phys. Chem. B* **2009**, *113*, 6378–6396. (b) The precise choice of the solvent in this model turns out to change all states with a nearly constant number (<1 kcal/mol variation in barrier heights). Therefore, the choice of a particular solvent is not critical for the overall outcome. We chose ACN as model to thus represent a highly acidic organic solvent.

(16) *Spartan'10*, Version 1.1.0; Wavefunction, Inc.: Irvine, CA, 2010.

(17) Wang, X.; Chen, R.-x.; Sue, A. C.-H.; Zuilhof, H.; Aquino, A. J. A.; Lischka, H. Introduction of polar or nonpolar groups at the hydroquinone units can lead to the destruction of the columnar structure of Pillar[5]arenes. *Comput. Theor. Chem.* **2019**, *1161*, 1–9.

(18) (a) Miyahara, Y.; Inazu, T.; Yoshino, T. Synthesis of [1.1.1.1]paracyclophane. *Tetrahedron Lett.* **1983**, *24*, 5277–5280.

(b) Kosiorek, S.; Rosa, B.; Boinski, T.; Butkiewicz, H.; Szymański, M. P.; Danylyuk, O.; Szumna, A.; Sashuk, V. Pillar[4]pyridinium: a square-shaped molecular box. *Chem. Commun.* **2017**, *53*, 13320–13323. (c) See for an overview of related compounds: Schneebeli, S. T.; Strutt, N. L.; Chang, C.; Stoddart, J. F. Pillararene-related Macrocycles. In *Pillararenes*; Ogoshi, T., Ed.; Monographs in Supramolecular Chemistry No. 18; The Royal Society of Chemistry, 2016.

(19) Santra, S.; Kovalev, I. S.; Kopchuk, D. S.; Zyryanov, G. V.; Majee, A.; Charushin, V. N.; Chupakhin, O. N. Role of polar solvents for the synthesis of pillar[6]arenes. *RSC Adv.* **2015**, *5*, 104284–104288.

(20) (a) Ogoshi, T.; Ueshima, N.; Akutsu, T.; Yamafuji, D.; Furuta, T.; Sakakibara, F.; Yamagishi, T.-a. The template effect of solvents on high yield synthesis, co-cyclization of pillar[6]arenes and interconversion between pillar[5]- and pillar[6]arenes. *Chem. Commun.* **2014**, *50*, 5774–5777. (b) Ogoshi, T.; Ueshima, N.; Sakakibara, F.; Yamagishi, T.-a.; Haino, T. Conversion from Pillar[5]arene to Pillar[6–15]arenes by Ring Expansion and Encapsulation of C<sub>60</sub> by Pillar[n]arenes with Nanosize Cavities. *Org. Lett.* **2014**, *16*, 2896–2899.

(21) (a) Nierengarten, I.; Meichsner, E.; Holler, M.; Pieper, P.; Deschenaux, R.; Delavaux-Nicot, B.; Nierengarten, J.-F. Preparation of

Pillar[5]arene-Based [2]Rotaxanes by a Stopper-Exchange Strategy. *Chem.—Eur. J.* **2018**, *24*, 169–177. (b) Nierengarten, I.; Guerra, S.; Holler, M.; Karmazin-Brelot, L.; Barberá, J.; Deschenaux, R.; Nierengarten, J.-F. Macrocyclic Effects in the Mesomorphic Properties of Liquid-Crystalline Pillar[5]- and Pillar[6]arenes. *Eur. J. Org. Chem.* **2013**, *2013*, 3675–3684. (c) Holler, M.; Allenbach, N.; Sonet, J.; Nierengarten, J.-F. The high yielding synthesis of pillar[5]arenes under Friedel–Crafts conditions explained by dynamic covalent bond formation. *Chem. Commun.* **2012**, *48*, 2576–2578.

(22) Mirzaei, S.; Wang, D.; Lindeman, S. V.; Sem, C. M.; Rathore, R. Highly Selective Synthesis of Pillar[n]arene (n = 5, 6). *Org. Lett.* **2018**, *20*, 6583–6586.

(23) Legault, C. Y. *CYLview20*; Université de Sherbrooke, 2020 (<http://www.cylview.org>).